Polyphosphazene Electrolytes. 1. Preparation and Conductivities of New Polymer Electrolytes Based on Poly[bis(amino)phosphazene] and Lithium Perchlorate

Y. W. Chen-Yang,* J. J. Hwang, and F. H. Chang

Department of Chemistry, Chung Yuan Christian University,
Chung-Li, Taiwan 32023, ROC

Received February 21, 1996; Revised Manuscript Received December 12, 1996[⊗]

ABSTRACT: Two series of new phosphazene polymer electrolytes, PPAP/$LiClO_4$ and PHAP/$LiClO_4$, were prepared by complexing lithium perchlorate, $LiClO_4$, to poly(bis(pentylamino)phosphazene), PPAP, and poly(bis(hexylamino)phosphazene), PHAP, respectively. The electrolytes were characterized by the combination of FTIR, ^{31}P-NMR, and ^{13}C-NMR spectroscopies. Films of these electrolytes showed good dimensional stability and ionic conductivity. The glass transition temperatures were determined by differential scanning calorimetry. The highest ionic conductivity, σ, was 7 orders higher in magnitude than the σ of its parent polymer and was similar to the σ of PEO at room temperature. The plots of ionic conductivity versus temperature for the polymer electrolytes were found to correspond to the Vogel−Tammann−Fulcher equation throughout the temperature range 30−100 °C.

Introduction

Solid polymer electrolytes have been extensively investigated during the past two decades due to their potential applications in high-energy density batteries, specific ion sensors, electrochromic displays, and other electrochemical devices.[1−8] Among them, a large number of studies have focused on the polymer-based poly(ethylene oxide)s, PEO, containing lithium salts, which are known as reference polymer electrolytes.[7,8] In order to meet the criteria for practical devices, such as batteries, conductivities in the range of 10^{-3}−10^{-6} S cm^{-1} are desired over a temperature range of ambient to 390 K. Many modifications, such as polymer blends and plasticizers, have been suggested to improve their conductivity and mechanical stability.[9−11] In addition, there are also many studies centered on preparing new solid polymer electrolytes with high conductivities and dimensional stabilities other than poly(ether oxide)s.[12−15] These include the polymers with more flexible backbones, such as polyphosphazene and polysiloxane, which have short polyether chains as pendent side groups.[12,16,17] Poly(bis((methoxyethoxy)ethoxy)phosphazene), MEEP, is one such material that combines the high ion-solvating property of its ethylene oxide side groups with the elastomeric character imparted by the flexible polyphosphazene backbone.[12] Although it shows high ionic conductivity, its poor mechanical stability is the disadvantage of this material for practical use. Therefore, chemical and radiation cross-linking methods have been applied to improve the mechanical properties.[19] Blonsky et al. indicated that amino-substituted ($NHCH_3$, $N(CH_3)_2$) polyphosphazene did not perform satisfactorily as an electrolyte.[18] In the present study, longer chain amine side groups were prepared, and their lithium salt complexes were found to give good conductivity and good mechanical stability at room temperature.

Experiment

1. Material. Hexachlorocyclotriphosphazene was kindly provided by the Nippon Fine Chemical Corp. Pentylamine, hexylamine, and triethylamine were purchased from Merck Chemical Co. Lithium perchloride ($LiClO_4$), tetrahydrofuran (THF), sulfur (S_8), and methanol were purchased from Aldrich Chemical Co. $LiClO_4$ was dried by vacuum (<10^{-4} Torr) for 24 h at 120 °C prior to use, and the THF was distilled under nitrogen from sodium benzophenone before use. All the other reagents and solvents were used as received.

2. Synthesis of Poly(dichlorophosphazene). The method described below was followed for the preparation of Poly(dichlorophosphazene), $(NPCl_2)_n$.[20] Hexachlorocyclotriphosphazene, $(NPCl_2)_3$, (50.0 g) and sulfur (5.0 g), used as a catalyst, were weighed directly into a Pyrex ampule. The ampule was evacuated to 0.05 Torr for 1 h and then sealed. The sealed ampule was placed in a furnace and heated to 285 °C until the clear melting mixtures became highly viscous but still slightly mobile. The ampule was opened, and the contents were extracted with dry benzene to remove the cross-linked polymer. The product, linear polymer $(NPCl_2)_n$, was then purified by precipitation from a benzene solution into *n*-hexane. An average of 50−60% conversion to the linear polymer was obtained.

3. Synthesis of Poly(bis(*n*-pentylamino)phosphazene) (PPAP). A method similar to that reported by Allcock et al.[21] was followed for the preparation of PPAP. A solution of poly(dichlorophosphazene) (25.0 g, 0.216 unit mol) in THF (400 mL) was added dropwise to a stirred solution of *n*-pentylamine (94.0 g, 1.08 mol) and triethylamine (65.7 g, 1.08 mol) in THF (800 mL). The reaction mixture was stirred at 25 °C for 14 h and then added to excess methanol to precipitate the polymer. Residual amine hydrochloride salt was removed by several washings with methanol. The polymer was then dried and further purified by reprecipitation from the THF solution into methanol. The residual solvent was finally removed by drying under a vacuum to give a polymer product (31.9 g, 68% yield).

4. Synthesis of Poly(bis(*n*-hexylamino)phosphazene) (PHAP). As in the synthesis of PPAP, similar reaction procedures were implemented for PHA. A solution of poly(dichlorophosphazene) (30.0 g, 0.259 unit mol) in THF (400 mL) was added dropwise to a stirred solution of *n*-hexylamine (130.0 g, 1.3 mol) and triethylamine (82.6 g, 0.819 mol) in THF (800 mL). The reaction mixture was stirred at 25 °C for 14 h before being added to the excess methanol to precipitate the polymer. Purification from salts and oligomers was effected by repeated precipitation from THF into methanol. The residual solvent was finally removed by drying under a vacuum to give a polymer product (41.2 g, 65% yield).

5. Preparation of Polymer−$LiClO_4$ Salt Electrolytes. The concentration of salt is expressed as the molar ratio of salt fed to a polyphosphazene repeat unit, $F = [LiClO_4]/[PN]$. In order to prepare the electrolytes, appropriate amounts of poly(aminophosphazene) were dissolved in a small amount of THF, and after the addition of the required quantity (F value)

[⊗] Abstract published in *Advance ACS Abstracts,* June 15, 1997.

S0024-9297(96)00289-6 CCC: $14.00

Table 1. Elemental Analysis Data of PPAP and PHAP

polymer		% N	% C	% H	% Cl
PPAP	cal	19.4	55.3	11.1	0.00
	exp	19.4	54.4	11.0	<0.1
PHAP	cal	17.1	58.8	11.4	0.00
	exp	17.2	57.9	11.2	<0.1

Scheme 1

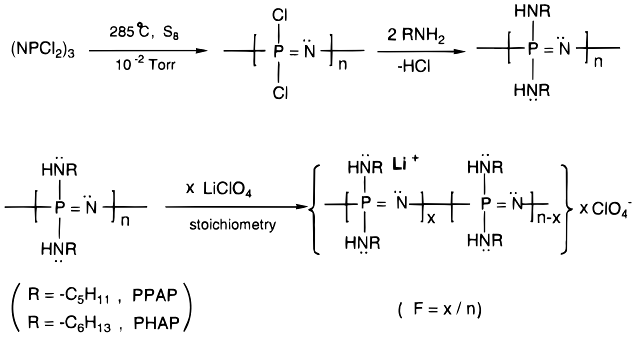

of the corresponding lithium salt, the solution was stirred well. The electrolyte films were prepared by casting the solution onto Teflon dishes. The films were allowed to dry at room temperature inside a nitrogen-filled glovebox. The thickness of the films varied between 0.01 and 0.02 cm. The dried films were stored inside the glovebox. The electrolytes with *F* = 0–0.4 were successfully prepared. Attempts to increase the *F* value were unsuccessful, since some precipitates began to appear in the solution under the condition used.

6. Instruments. The ^{31}P-NMR spectra were measured on a Bruker AC 200 spectrometer and $N_3P_3Cl_6$ assigned to 20 ppm was used as a reference for ^{31}P-NMR. ^{1}H-NMR spectra were measured on a Varian Unity 400 spectrometer. As usual, $CDCl_3$ was used as a reference for ^{1}H-NMR. The FTIR spectra were recorded on a Biorad-Digilab FTS-7. The samples were sandwiched between two KBr windows. DSC measurements were implemented with a Seiko DSC 200. Typically, the samples were heated first at a rate of 10 °C/min to 150 °C and immediately cooled back to the initial temperature. This was followed by another heating cycle to study possible thermal hysteresis. The ionic conductivities of the polymer electrolytes were measured by the complex impedance method using an SI 1260 impedance/gain-phase analyzer over a frequency range of 10^{-5}–10^6 Hz, a temperature control unit, QUATRO, with a temperature range of −196 to +300 °C.

Results and Discussion

Preparation of the Polymer Electrolytes. The poly(bis(amino)phosphazene)s, PPAP and PHAP, and the corresponding solid electrolytes, PPAP/$LiClO_4$ and PHAP/$LiClO_4$, were prepared according to Scheme 1.

The results of elemental analysis, FTIR and ^{1}H NMR spectra of PPAP and PHAP shown in Table 1 and Figures 1 and 2 indicate that the PPAP and PHAP prepared were pure poly(bis(amino)phosphazene)s with the expected structures.

The FTIR spectra in Figure 1 also show that the polymer electrolyte samples prepared were water-free. In addition, it was found that the films prepared were all homogenous free-standing films with good dimensional stability. The clarity of the films was found to depend upon the amount of salt present. The films prepared from the polyelectrolytes with $F < 0.3$ were transparent, and those with $F > 0.3$ were opaque. This implies that the polymer matrix and the lithium salt are miscible in both PPAP/$LiClO_4$ and PHAP/$LiClO_4$ electrolytes with a small *F* value and are partially immiscible when the salt content is increased. After the addition of lithium perchlorate, the electrolytes formed had less solubility than their parent polymers. The electrolytes were slightly insoluble in chloroform and partially soluble in tetrahydrofuran and dichloromethane, although they were all good solvents for their parent polymers, PPAP and PHAP. An attempt to use PPA, poly(bis(propylamino)phosphazene), and PBA, poly(bis-

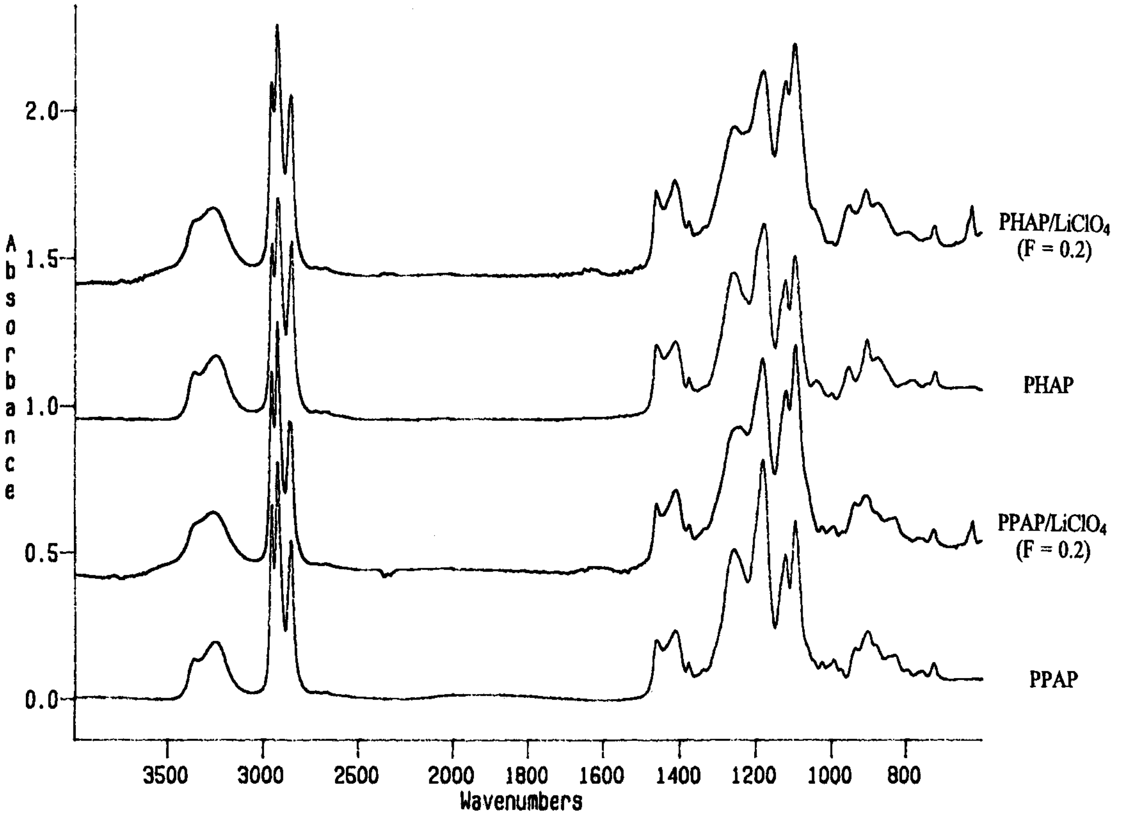

Figure 1. FTIR spectra of PPAP/$LiClO_4$ and PHAP/$LiClO_4$ electrolytes at various *F* values.

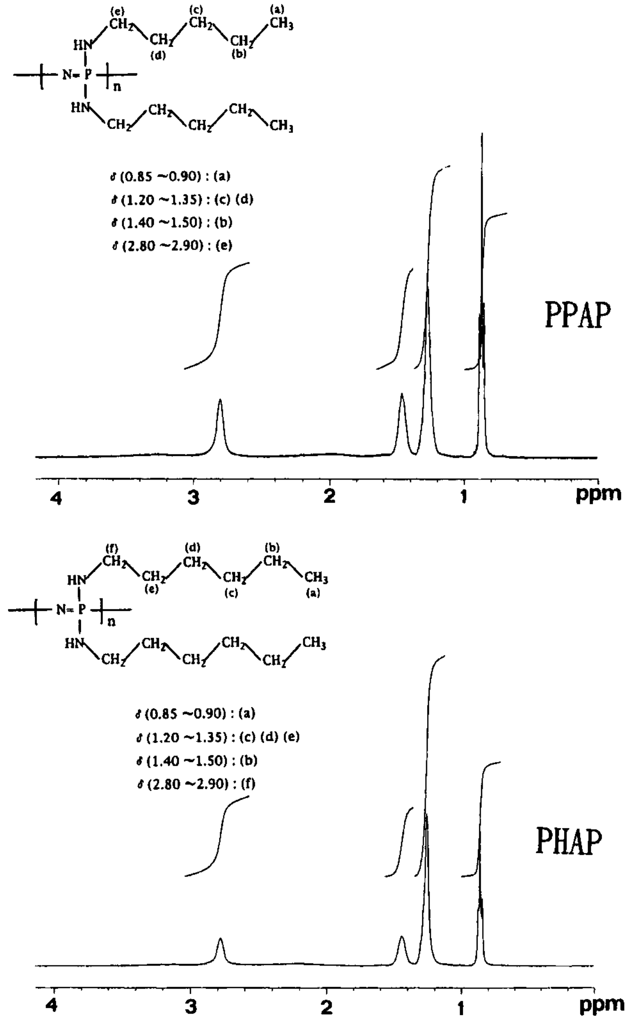

Figure 2. ^{1}H NMR spectra of PPAP and PHAP in $CDCl_3$ solvent.

(butylamino)phosphazene), to prepare the corresponding electrolytes was unsuccessful due to the poor solubility of the salts in the solvents, which could dissolve PPA and PBA.

Interaction of the Polymer and the Salt. It is known that the etheric phosphazene polymer–salt adducts, such as MEEP/$LiClO_4$, are formed by solvation of the polar oxygen in the ether side chains and the metal salts and that they exhibit good ionic conductivities.[12] On the other hand, the coordination of poly(bis(methylamino)phosphazene) with $PtCl_2$ is considered to involve the backbone nitrogen atoms rather than the methylamino side groups and is known as an antitumor polymer drug.[22,23] Nevertheless, in the present researchers previous study,[24] it was found that a coordination between the silver cation and the nitrogens on both the backbone and the side chains occurred in the poly(bis(propylamino)phosphazene)–$AgNO_3$ and poly(bis(*n*-butylamino)phosphazene)–$AgNO_3$ complexes. These results indicate that the interaction site of the polyphosphazene and metal salts may depend on the basicity of the potential coordinating atom and the hard/soft character of the salt ions. Therefore, it is interesting to investigate the possible interaction between the poly(bis(amino)phosphazene) and the lithium salt used in this study. A combination of FTIR, ^{31}P-NMR, and ^{13}C-NMR spectroscopy measurements were performed, and the results are discussed below.

The FTIR spectra for PPAP/$LiClO_4$ electrolytes and that of their parent polymer PPAP demonstrated that the intensities and the peak frequencies of the characteristic absorptions, 1257 cm^{-1} for P=N stretching and 906 cm^{-1} for P–N–C stretching, predominantly remain unchanged, indicating that the interaction between the backbone nitrogen and lithium is not revealed in the spectra. The bands in the region 3000–3400 cm^{-1} are assigned to the N–H stretchings. As listed in Table 2, it was seen that the addition of lithium salt leads to an increase in frequency for the band at higher frequency levels, indicating a change concerning the interaction of the N–H groups. In order to better understand this change, the absorption in the region was band-fitted using "Bandfit" software, a facility of the Bio-Rad spectrometer, separating the N–H mode into three contributions for PPAP/$LiClO_4$ system. As seen in Figure 3a for the $F = 0.2$ complex, the bands peaking at ~3366 and ~3254 cm^{-1} are assigned to the free N–H stretching and the hydrogen-bonding N–H stretching, respectively, as in the PPAP spectrum in Figure 3b. The decrease in the absorbance of the hydrogen-bonding N–H stretching with the addition of salt indicates that a portion of the hydrogen bonding of the N–H group is being disrupted. The middle band peaking at ~3310 cm^{-1} is, on the other hand, referred to the lithium ion solvated N–H stretching. This implies an interaction of the side chain nitrogen with the lithium ion. A similar change was also found in the FTIR spectra of the PHAP/$LiClO_4$ system.

As can be observed in Figure 4, in each ^{31}P-NMR spectrum of the PPAP/$LiClO_4$ electrolytes, the principal peak position has very little shift relative to the peak of the parent polymer and a small new peak is found at the lower field of the main peak. The data listed in Table 3 suggest that most of the phosphorus atoms are not affected by the salt, i.e., the interaction between the backbone nitrogen atoms and lithium ions is negligible, and only a small portion of the phosphorus atoms are slightly deshielded by the amino groups that are solvating with the lithium ions, as suggested by the FTIR spectra.

In addition, the ^{13}C-NMR spectrum was also measured to obtain more information concerning the interaction between side-chain nitrogen and the lithium ion.

Table 2. Characteristic Absorptions in FITR Spectra of PPAP, PHAP, and the Electrolytes (in cm^{-1})

sample	*F* value	N–H	C–H	P=N	C–N	P–N–C
PPAP	0	3253, 3353	2927, 1414	1257	1178, 1095	906
PPAP/$LiClO_4$	0.1	3253, 3363	2927, 1414	1257	1178, 1092	906
PPAP/$LiClO_4$	0.2	3253, 3367	2927, 1414	1257	1178, 1092	906
PPAP/$LiClO_4$	0.3	3253, 3369	2927, 1414	1257	1178, 1092	906
PPAP/$LiClO_4$	0.4	3253, 3369	2926, 1414	1257	1178, 1092	906
PHAP	0	3247, 3351	2924, 1412	1257	1180, 1095	905
PHAP/LilO4	0.1	3247, 3353	2924, 1412	1257	1180, 1096	905
PHAP/$LiClO_4$	0.2	3247, 3358	2924, 1412	1257	1180, 1097	905
PHAP/$LiClO_4$	0.3	3247, 3362	2924, 1412	1257	1180, 1097	905
PHAP/$LiClO_4$	0.4	3247, 3363	2924, 1412	1257	1180, 1098	905

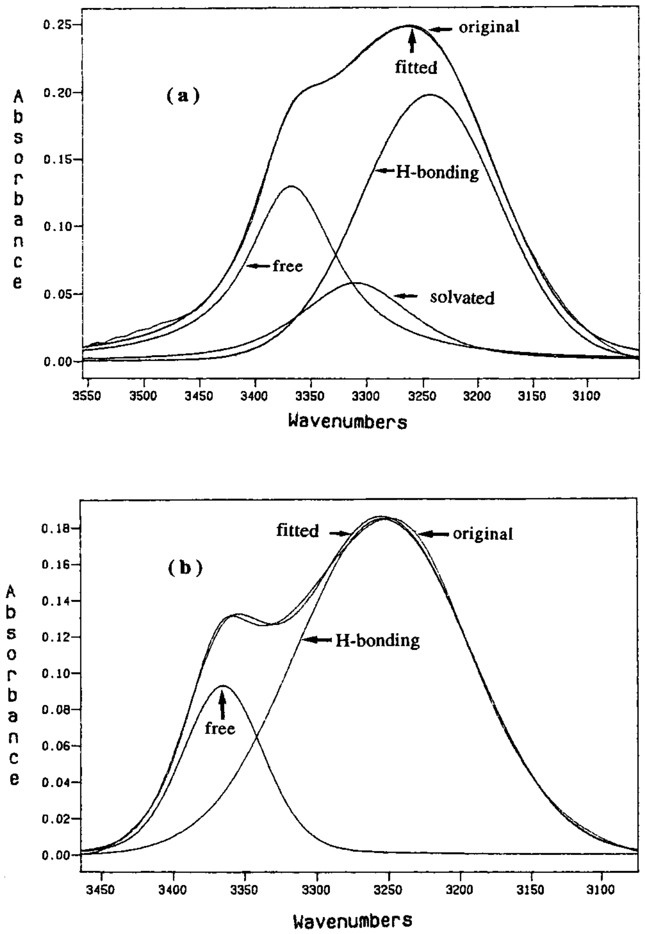

Figure 3. Band fittings in the ν(N−H) FTIR region for (a) PPAP−LiClO$_4$ (F = 0.2) and (b) PPAP.

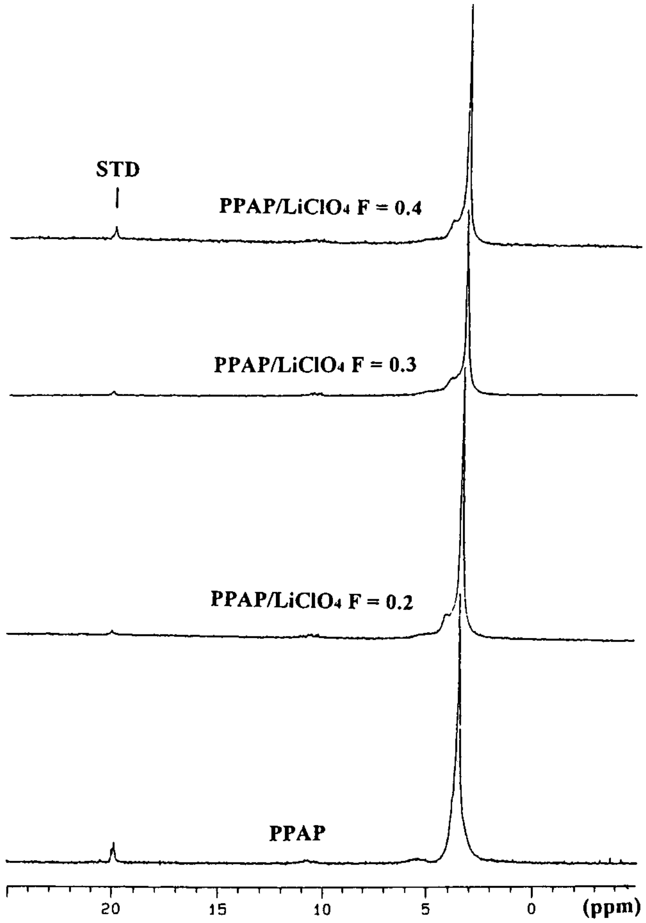

Figure 4. ^{31}P NMR spectra of PPAP/LiClO$_4$ electrolytes at various F values in CDCl$_3$ solvent. STD: (NPCl$_2$)$_3$ as an internal standard.

Table 3. ^{31}P NMR Data of PPAP, PHAP, and the Electrolytes (in ppm)

	F value					
sample	0	0.1	0.2	0.3	0.4	0.5
PPAP/LiClO$_4$	3.57	3.52	3.23	3.17	3.27	3.22
PHAP/LiClO$_4$	3.73	3.64	3.62	3.61	3.57	3.62

Table 4. ^{13}C NMR Chemical Shifts of PPAP, PHAP, and the Electrolytes with F = 0.2 (in ppm)

	sample			sample	
atom position	PPAP	PPAP/ LiClO$_4$	atom position	PHAP	PHAP/ LiClO$_4$
C$_1$	41.5	41.5	C$_1$	41.6	41.6
C$_2$	31.8	31.7	C$_2$, C$_4$	32.1	31.8
C$_3$	29.7	29.5	C$_3$	27.4	27.0
C$_4$	22.7	22.6	C$_5$	22.8	22.7
C$_5$	14.1	14.0	C$_6$	14.1	14.0

It was found that although the peaks were slightly broader, the peak positions all remained almost the same, as listed in Table 4. This suggests that the magnetic environment of the carbons is scarcely influenced by the presence of lithium ions.

As discussed above, the results of the FTIR and the NMR measurements indicated that, as in the MEEP/LiClO$_4$ system, the interaction between the poly(aminophosphazene) and lithium perchlorate was predominantly solvated with the polar atoms of the side chain, nitrogens, in the poly(aminophosphazene)/LiClO$_4$ electrolytes prepared in this study.

DSC Measurements. Figure 5 displays the DSC thermograms of the PPAP/LiClO$_4$ system with F = 0−0.4. It is apparent that the thermograms of the electrolytes with $F < 0.25$ predominantly exhibit a glass transition temperature, indicating that these electrolytes are amorphous by incorporating LiClO$_4$ and that LiClO$_4$ is miscible in the polymer in these samples as discussed above. However, another phase is gradually formed with increasing salt content at around 70 °C. The electrolyte with F = 0.25 exhibits several interesting features, including a glass transition at −17 °C, which corresponds to the amorphous phase formed by the solvation of LiClO$_4$ in a PPAP matrix, as found in the cases with $F < 0.2$, a second and more obvious glass transition at about 70 °C, and a very prominent melting endotherm occurring at approximately 146 °C, which is also found in the thermogram of the LiClO$_4$ salt. This behavior indicates that the electrolyte is multiphased, with at least two distinct amorphous phases with different LiClO$_4$ concentrations and a possible LiClO$_4$ ion-pair crystalline region. The weak glass transition phase, which has T_g at a somewhat higher temperature than the T_g for pure PPAP, is attributed to the solvation of LiClO$_4$ in a PPAP matrix, as observed in the cases with $F < 0.2$. The second glass transition phase with a much higher T_g value, on the other hand, suggests that the phase is richer in salt. This phase, however, became crystalline as the salt content was further increased, as shown by the endothermal peak found at approximately 82 °C for the electrolytes with $F > 0.3$, causing a reduction in the ionic conductivity, which is discussed later in this report.

For the PHAP/LiClO$_4$ system, the thermogram of the parent polymer PHAP in Figure 6 shows an endotherm

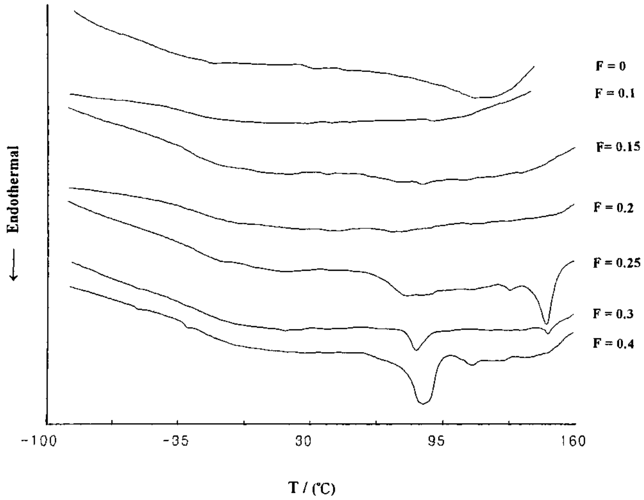

Figure 5. DSC heating curves recorded at 10 °C/min in the PPAP/LiClO$_4$ electrolyte system.

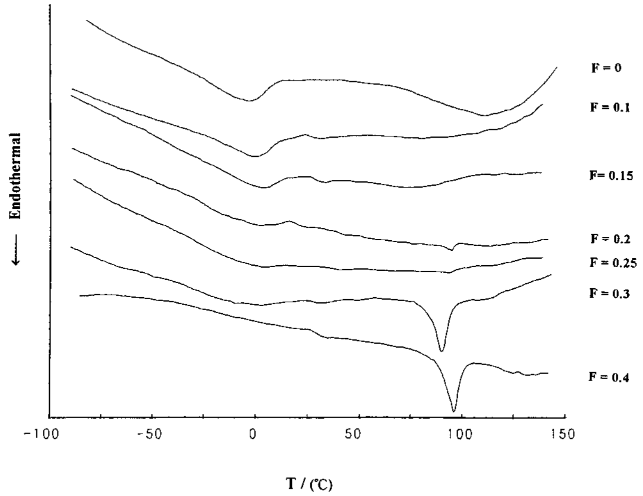

Figure 6. DSC heating curves recorded at 10 °C/min in the PHAP/LiClO$_4$ electrolyte system.

Table 5. Glass Transition Temperatures (T_g) of PPAP, PHAP, and the Electrolytes in (°C)

sample	*F* value 0	0.1	0.15	0.2	0.25
PPAP/LiClO$_4$		−34	−25	−25	−17, 70
PHAP/LiClO$_4$	−4	+1	+3	+4	−2

peak at approximately 0 °C, revealing a partially crystalline phenomenon. With the incorporation of LiClO$_4$ in the PHAP, the degree of crystallinity is decreased and the melting peaks completely disappear when $F = 0.25$. In addition, similar to the PPAP/LiClO$_4$ system, a crystalline phase is also found at approximately 95 °C when the *F* value is larger. The DSC results suggest that the electrolytes with an *F* value less than 0.3 are basically amorphous in the temperature range of interest.

As listed in Table 5, the T_g is increased slightly with an increasing salt content for both systems. The small increase in the glass transition temperature supports the supposition that the ion−polymer interaction is a weak solvation, as inferred above. In addition, the T_g's of the PPAP system are all lower than that of the PHAP system with the same *F* value. This means that the PPAP system has higher flexibility at room temperature and may transport ions more easily than the PHAP system, as discussed below.

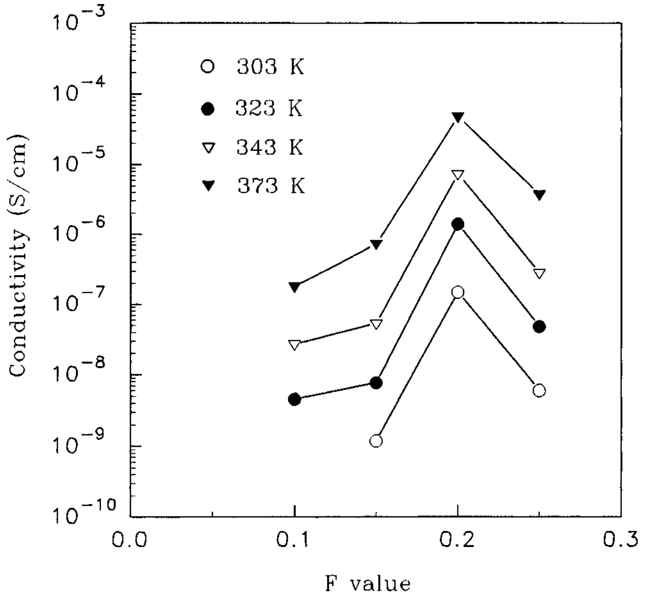

Figure 7. Isothermal variations of ionic conductivity with LiClO$_4$ concentration in PPAP/LiClO$_4$ electrolytes.

Table 6. Conductivities, σ, of PPAP/LiClO$_4$ and PHAP/LiClO$_4$ (in S cm^{-1})

temp (°C)	*F* value 0[a]	0.1	0.15	0.2	0.25
			PPAP/LiClO$_4$		
30	4.0×10^{-14}		1.2×10^{-9}	1.5×10^{-7}	6.0×10^{-9}
50		$4.5 \times 10{-}^{9}$	7.7×10^{-9}	1.4×10^{-6}	4.8×10^{-8}
70		2.7×10^{-8}	5.3×10^{-8}	7.3×10^{-6}	2.8×10^{-7}
100		1.8×10^{-7}	7.3×10^{-6}	4.8×10^{-5}	3.7×10^{-6}
			PHAP/LiClO$_4$		
30	1.6×10^{-13}			2.2×10^{-8}	
50		3.3×10^{-9}	3.9×10^{-9}	1.9×10^{-7}	1.3×10^{-8}
70		1.8×10^{-8}	2.2×10^{-8}	1.1×10^{-6}	7.3×10^{-8}
100		1.5×10^{-7}	1.9×10^{-8}	6.6×10^{-6}	1.2×10^{-6}

[a] The conductivity was measured by the four-probe method.[34]

Ionic Conductivity. The conductivities of the films prepared were obtained from the impedance measurements.[5,25] A Cole−Cole plot of the impedance data, Z' vs Z'', which represent the real part and the imaginary part, respectively, at the test temperature indicated a depressed semicircle with a spur at the low frequencies. The ionic conductivity, σ, was then calculated using the value of the bulk resistance, R_b, as determined from the interception of the spur at the real Z' axis, the thickness of the electrolyte film, *L*, and the area of the electrodes, *A*, according to the following formula.

$$\sigma = 1/R_b(L/A)$$

As reported previously,[26] all the pure poly(bis(amino)phosphazene)s have conductivities in the low range of 10^{-11}−10^{-15} S cm^{-1} at room temperature, indicating an insulating characteristic. It was found that after the addition of lithium perchlorate salt, the conductivities of both the PPAP/LiClO$_4$ and the PHAP/LiClO$_4$ systems prepared in this study were significantly increased. A comparison of the dependence of ionic conductivity on salt concentration for the two systems obtained from the impedance measurements described above is shown in Figure 7, and Table 6 and indicates that the conductivities are increased 5−7 orders in magnitude at 30 °C.

The data reveal that LiClO$_4$ undergoes dissociation in the polymer matrix by solvation as suggested above, and the conductivity depends on the salt concentration.

The ionic conductivities initially increase as the salt content is increased, due to the increase in the number of charge carriers, and reach a maximum around an *F* value of 0.2. A further increase in salt content leads to the formation of less mobile ion pairs or ionic aggregates and, therefore, a decrease in the conductivity value. A similar result is generally observed for most of the polymer salt electrolytes.[27-29] This behavior is consistent with the phenomena found in the DSC analysis described above, in which a crystalline phase is formed for the polymer electrolytes with $F > 0.3$, which can cause a low ionic mobility. The maximum conductivity of PPAP/$LiClO_4$ with $F = 0.2$ at room temperature is 1.5×10^{-7} S cm^{-1}, which is about the same as that for the PEO systems, a well-known reference solid polymer electrolyte system,[30,31] but lower than that for the sticky polyphosphazene electrolyte MEEP/$LiClO_4$.[12] Similarly, a maximum value was obtained for the PHAP/$LiClO_4$ with $F = 0.2$ at room temperature. However, the conductivity values obtained for a PHAP/$LiClO_4$ system are all lower than those for a PPAP/$LiClO_4$ system with the same *F* value. This may be ascribed to the lower ionic mobility due to a higher T_g.

Temperature Variation in Conductivity. The temperature dependence of the ionic conductivity of the electrolytes was measured from 30 to 100 °C. The data at 30, 50, 70, and 100 °C are listed in Table 6. It is clear that the PPAP/$LiClO_4$ with $F = 0.2$ is the most promising of the system studied. Its conductivity reached values in the order of 10^{-7} S cm^{-1} at 30–50 °C, 10^{-6} S cm^{-1} at 50–80 °C, and 10^{-5} S cm^{-1} at 80–100 °C. In this temperature range the conductivities of the system with PPAP are all about 1 order of magnitude higher than those for the analogous system with PHAP. Since the films with $F < 0.25$ are all amorphous polymeric electrolytes without any crystalline regions, the Vogel–Tamman–Fulcher (VTF) empirical equation, used to characterize the viscoelastic properties of polymer systems, was used to analyze the conductivity data obtained in this study. The thermodynamic glass transition temperature T_o values were calculated by subtracting 50 K from their T_g values, as predicted by the Adams–Gibbs configurational entropy model.[32,33]

$$\sigma = \sigma_o \exp(-B/T - T_o)$$

$$T_o = T_g - 50$$

Figures 8 and 9 indicate that the temperature dependence of the conductivities in the temperature range measured has a good correspondence to the VTF approximation, revealing that segmental movement and, therefore, ionic mobilities may be explained by simple configurational entropy arguments. The pre-exponential factors, σ_o, and pseudoactivation energies, *B*, obtained from the plots are listed with T_o values in Table 7. It is obvious that σ_o and *B* values of the PPAP system are all larger than that of the PHAP system.

Conclusion

Two new series of dimensionally stable polymer electrolytes based on poly(bis(amino)phosphazene)s, PPAP and PHAP, with lithium perchlorate were prepared. It was found that the interaction between the polymer matrix and the salt was a weak solvation principally through the nitrogen atoms on the side chain and the lithium ions. The polymer electrolytes obtained were completely amorphous when the *F* value was less than 0.25 at the temperature of interest. The ionic conductivity was increased with an increasing salt content and was in the range of 10^{-9} and 10^{-5} S cm^{-1} between 30 and 100 °C. It is noteworthy that the ionic conductivity was found to be 1 order higher in the polymer electrolytes with PPAP than in those with PHAP. The segments in the PPAP/$LiClO_4$ polyelectro-

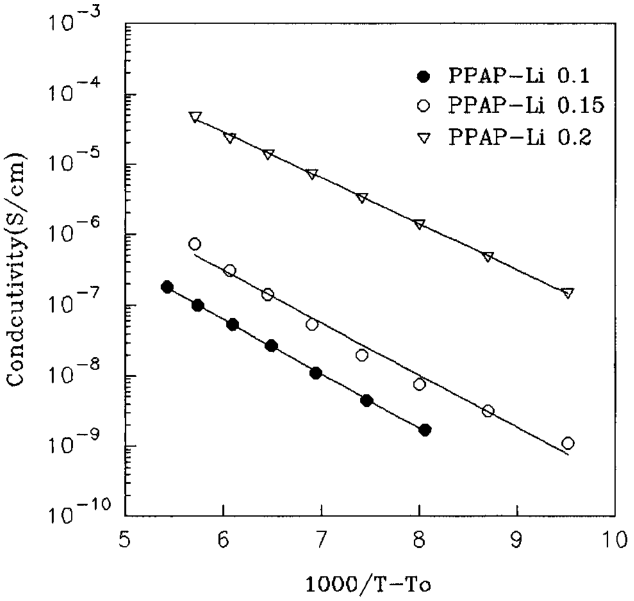

Figure 8. VTF-plotted approximation of conductivity vs reciprocal temperatures in PPAP/$LiClO_4$ electrolytes at various *F* values.

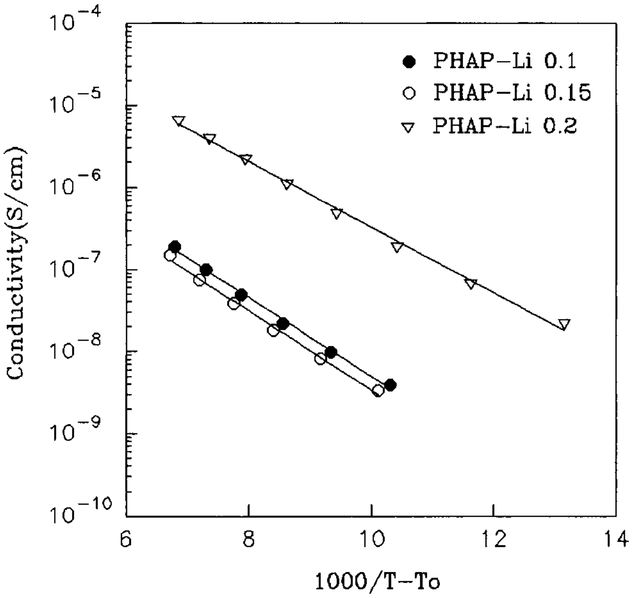

Figure 9. VTF-plotted approximation of conductivity vs reciprocal temperatures in PHAP/$LiClO_4$ electrolytes at various *F* values.

Table 7. VTF Parameters of PPAP/$LiClO_4$ and PHAP/$LiClO_4$

	$F = 0.1$	$F = 0.15$	$F = 0.2$	$F = 0.25$
		PPAP/$LiClO_4$		
B (K)	737	777	648	651
σ_o (S/cm)	8.1×10^{-3}	2.9×10^{-3}	0.220	2.2×10^{-2}
T_o (K)	189	198	198	206
		PHAP/$LiClO_4$		
B (K)	485	482	398	538
σ_o (S/cm)	2.4×10^{-4}	3.3×10^{-4}	3.2×10^{-3}	2.7×10^{-3}
T_o (K)	224	226	227	221

lytes are probably more flexible than those in the PHAP/$LiClO_4$ polyelectrolytes, as indicated by the lower T_g values, suggesting that the ionic mobility is assisted by the flexibility in the polymer matrix. The PPAP/$LiClO_4$ with $F = 0.2$, having a conductivity of 1.5×10^{-7} S cm^{-1} at room temperature and 4.8×10^{-5} S cm^{-1} at 100 °C, similar to the PEO/$LiClO_4$ system, is the most promising one in this study. In the temperature range 30−100 °C, the temperature dependence of the conductivities of the electrolytes follows the VTF empirical equation. The favorable ionic conductivity and dimensional stability make these polymer electrolytes possible candidates for solid polymer materials in rechargeable batteries and electrochromic devices.

Acknowledgment. The authors wish to thank the National Science Council of the ROC for the financial support of this work under the project NSC 84-2113-M-033-003 and Nippon Fine Chemical Co., Japan, for providing the hexachlorotriphosphazene.

References and Notes

(1) Armand, M. *Solid State Ionics* **1994**, *69*, 309.
(2) Abraham, K. M.; Alamgir, M. *Solid State Ionics* **1994**, *70/71*, 203.
(3) Gores, H. J.; Barthel, J. M. G. *Pure Appl. Chem.* **1995**, *67*, 919.
(4) Mani, T.; Stevens, J. R. *Polymer* **1992**, *33*, 834.
(5) Gray, F. M. *Solid Polymer Electrolytes: Fundamentals and Technological Application*; VCH: New York, 1991.
(6) Goodenough, J. B.; Manthiram, A.; Wnetrzewski, B. *J. Power Sources* **1993**, *43−44*, 269.
(7) Fenton, D. E.; Parker, J. M.; Wright, P. V. *Polymer* **1973**, *14*, 589.
(8) Wright, P. V. *J. Polym. Sci., Polym. Phys. Ed.* **1976**, *14*, 955.
(9) Abraham, K. M.; Alamgiv, M.; Reynolds, R. K. *J. Electrochem. Soc.* **1989**, *136*, 3576.
(10) Rawsky, G. C.; Fujinami, T.; Shriver, D. F. *Chem. Mater.* **1994**, *6*, 2208.
(11) Abraham, K. M.; Alamgir, M.; Moulton, R. D. *J. Electrochem. Soc.* **1991**, *138*, 921.
(12) Blonsky, P. M.; Shriver, D. F.; Austin, P.; Allcock, H. R. *J. Am. Chem. Soc.* **1984**, *106*, 6854.
(13) Kim, D. W.; Park, J. K.; Gong, M. S. *J. Polym. Sci., Part B: Polym. Phys.* **1995**, *33*, 1323.
(14) Gray, F. M.; MacCallum, J. R.; Vincent, C. A. *Macromolecules* **1988**, *21*, 392.
(15) Abraham, K. M.; Alamgir, M.; Reynolds, R. K. *J. Electrochem. Soc.* **1989**, *136*, 3577.
(16) Tada, Y.; Sato, M.; Takeno, N.; Nakacho, Y.; Shigehara, K. *Chem. Mater.* **1994**, *6*, 27.
(17) Zhou, G. B.; Khan, I. M.; Smid, J. *Macromolecules* **1993**, *26*, 2202.
(18) Blonsky, P. M.; Shriver, D. F.; Austin, P.; Allcock, H. R. *Solid State Ionics* **1986**, *18/19*, 258.
(19) Allcock, H. R. *Chem. Mater.* **1994**, *6*, 1476.
(20) Kajiwara, M.; Moriya, K.; Tomii, K.; Yano, S. *Makromol. Chem.* **1992**, *193*, 435.
(21) Allcock, H. R.; Cook, W. J.; Mack, D. P. *Inorg. Chem.* **1972**, *11*, 2584.
(22) Allcock, H. R.; Allen, R. W.; O'Brien, J. P. *J. Am. Chem. Soc.* **1977**, *99*, 3984.
(23) Allen, R. W.; O'Brien, J. P.; Allcock, H. R. *J. Am. Chem. Soc.* **1977**, *99*, 3987.
(24) Chen-Yang, Y. W.; Hwang, J. J.; Kau, J. Y. *J. Polym. Soc., Part A: Polym. Chem.* **1997**, *35*, 1023.
(25) Ratner, M. A.; Shriver, D. F. *Chem. Rev.* **1988**, *88*, 109.
(26) Hayashi, T.; Saito, H. *Bull. Chem. Soc. Japn.* **1977**, *50*, 1023.
(27) Florjanczyk, Z.; Krawiec, W.; Wieczorek, W.; Siekierski, M. *J. Polym. Sci., Part B: Polym. Phys.* **1995**, *33*, 1657.
(28) Li, J.; Pratt, L. M.; Khan, I. M. *J. Polym. Sci., Part A: Polym. Chem.* **1995**, *33*, 1657.
(29) Whang, W. T.; Lu, C. L. *J. Appl. Polym. Sci.* **1995**, *56*, 1635.
(30) Besher, S.; Vallee, A.; Bouchard, G.; Prud'homme, J. *Macromolecules* **1992**, *25*, 6480.
(31) Robitaille, C. D.; Fauteux, D. *J. Electrochem. Soc.* **1986**, *133*, 315.
(32) Adam, G.; Gibbs, J. H. *J. Chem. Phys.* **1965**, *43*, 139.
(33) Bruce, P. G.; Vincent, C. A. *J. Chem. Soc., Faraday Trans.* **1993**, *122*, 131.
(34) Elsenbaumer, R. L.; Shacklette, L. W. *Handbook of Conducting Polymer*, Skothein, T. A., Ed.; Marcel Dekker Inc.: New York, 1986; Vol. I, p 224.

MA960289Y